SolarPACES 2024, 30th International Conference on Concentrating Solar Power, Thermal, and Chemical Energy Systems

Al in Concentrating Solar Technology

https://doi.org/10.52825/solarpaces.v3i.2311

© Authors. This work is licensed under a Creative Commons Attribution 4.0 International License

Published: 22 Oct. 2025

Real-Time Image Enhanced Data-Driven Digital Twin (Real-TIME 3DT) for Flux Density Measurements

A Novel Non-Disruptive Universal Approach

Sergio Díaz Alonso^{1,*} , Christian Raeder¹, Kai Wieghardt¹, and Bernhard Hoffschmidt^{2,3}

¹Institute of Solar Research, German Aerospace Center (DLR), Im Langenbroich 13, 52428 Jülich, Germany ²RWTH Aachen University, Chair of Solar Components (DLR), Aachen, Germany ³German Aerospace Center (DLR), Linder Höhe, 51147 Köln, Germany

*Correspondence: Sergio Díaz Alonso, sergio.diazalonso@dlr.de

Abstract. Concentrated solar power (CSP) plants are considered one of the most attractive renewable energy producers (used for green fuel and electric power). Consequently, it is essential to enhance the different elements of their power cycles, especially the central receiver and the heliostat field. To achieve this, flux density measurement (FDM) is highly recommended. In this work, a novel methodology for FDM is presented, based on the usage of realtime data-driven simulation models in parallel with the traditional camera methods for the realtime enhancement of the results. In order to improve the output, a graph neural network is used, giving as a result a Real-Time Image-Enhanced Data-Driven Digital Twin (Real-TIME 3DT). All the data are obtained from a pre-existing data platform, where the signals from the sensors of the power plant are logged and stored. This way, it is possible to operate the model manually, or to let it work automatically with these sensors' outputs. Latencies smaller than 10 seconds are achieved and the results from the digital twin showed coherence, easy handling and great inter-operability with the neural network enhancement. On the Al-enhancement's side, the suppression of up-to 80% of the inaccuracies can be expected under parametrically semi-controlled conditions. Further work is being performed in Solar Tower Jülich (STJ) in order to contrast these results against real experimental measurements.

Keywords: Flux Density Measurement (FDM), Digital Twin, Machine Learning, Concentrating Solar Power, Renewable Energies

1. Introduction

Concentrated solar power (CSP) plants are one of the potential key players in the energy transition. They are not only used for power or heat production [1], but also for fuel synthesis [2]. In this context, the highest expectations are focused on Fresnel or Parabolic Trough plants for industrial low temperature heat production (at least in terms of commissioned and finished projects [3]) or Solar Power Tower (SPT) plants for thermochemical processes [4] or hybridization [5]. This last configuration can also be used with the first type of plants mentioned. However, efficiencies, costs, and reliability should be improved to increase the attractiveness of the technology for the society and investors. Regarding SPT systems, one of the main existing constraints is the universal, continuous, accurate, and non-disruptive flux density measurement (FDM) [6]. Furthermore, some of the most important operation parameters depend, to some extent, of the correct measurement of the solar input. Some examples are the sun-to-

power efficiency, the time availability of the plant (continuous operation), as well as the number of cycles and expenses for operation and maintenance (O&M). Therefore, it is possible to address a correlation between the FDM and the broader introduction of CSP in the market.

Flux density monitoring importance has led to multiple approaches summarized by Röger et al. [6] and mostly classified in direct and indirect methods. These procedures are often used to obtain the superposed flux distributions reflected by several heliostats within the central receiver surface. Direct methods leverage the usage of flux gauges (radiometers or calorimeters) to determine the flux values at their specific locations and to interpolate the intermediate values [7]. High costs and complex maintenance routines are required with these methods. Indirect methods utilize the reflection off the central receiver [8] or off additional Lambertian targets [9-11] to determine the incoming flux through the usage of CCD or CMOS cameras. The main drawbacks of these methods are the additional costs and complexity of the Lambertian structures (either fixed or mobile), the operation disruptions during scans, and the high uncertainties (up to 40%) when the reflection is measured off the receiver. Other approaches aim to measure individual heliostat's spots to later aggregate them computationally [12] or to use deep-learning methods to infer them from individual heliostats' beam training images [13]. Those methods lack applicability for industrial environments with numerous heliostats. The authors additionally address a literature gap in the usage of deep learning methods for superposed flux densities inference, as well as the usage of digital twinning in SPT systems.

The authors present a novel methodology based on the combination of state-of-the-art camera methods and the first real-time CSP digital twin (DT) supervised by Deep Learning algorithms. Firstly, the DT of the Solar Tower Jülich (STJ) has been developed in Python, backed-up by the real-time data acquisition from the pre-existing standardized 4.0 data platform located there [14]. Then, a machine-learning-guided correction module based on the systematic comparison between simulations and indirect methods' measurements is implemented, in order to generate a robust DT with lower uncertainties. Due to the lack of realistic measurements and the wide range of combinations the neural net has to deal with, synthetic superposed flux data (sim2sim) are also used as a pre-training of the Deep Learning enhancing algorithm. The results of this pre-training are presented hereafter. The main aim of this project is to go beyond the constraints mentioned in the paragraph above, these precepts being the basis of the design.

2. Methodology

In this design, a systematic methodology is presented for the universal, continuous and non-disruptive measurement of flux density in central receivers of SPT plants. The computational part of this work consists of a library of flexible Python scripts, configurable according to the parameters of the solar tower the user wants to study (either on design or operation stages) and the "ad-hoc" configuration for the Solar Tower Jülich (STJ). There are mainly two types of scripts according to the task they fulfil:

- 1. Digital twin. This set of Python scripts aims to the connection with the data platform and the querying (get, post, delete or patch) requests according to the operator instructions. Furthermore, there are also different functions for the automatic definition of the synchronous and asynchronous parameters of the corresponding solar plant (check chapter 2.1.).
- 2. Machine (deep) learning correction. This set of functions is composed by the neural network itself (U-Net). Moreover, there are some auxiliary scripts in order to define the data pipeline, as well as the ray-level correction, usable for cavity receivers in the future.

At the same time, a state-of-the-art camera method (e.g. "Scan Method" [8]) is configured to monitor the central receiver aperture plane in real-time, at least during the training process of the deep learning module (check Figure 1). This way, it will be possible to get high quality

(state of the art accuracy) ground truth images in order to train the neural network. When the system is calibrated and the U-Net is trained, the FDM camera method is not used until the following calibration. The calibration has to be performed only when the characteristics of the heliostats or the central receivers have changed drastically, so the result is an extremely unsupervised system with long duty cycles. The camera method is selected according to the features of the measurement to be performed, as the Scan Method is not the only option. For example, it is also possible to capture grayscale images from Lambertian targets located at the receivers' aperture plane under superposed flux situations, analogous to camera-target method. This option simplifies the usage of this methodology for cavity receivers or complex geometries.

The aim of this approach is the possibility of obtaining state-of-the-art quality results from simulations, in order to imitate this level of accuracy avoiding interruptions of the plant operation, as well as intensive maintenance. Furthermore, it is possible to get real-time supervision for cavity receivers looking at the aperture plane and at the radiation shield with the accuracy of the current methods and, again, without interfering in the operation of the cavity receivers.

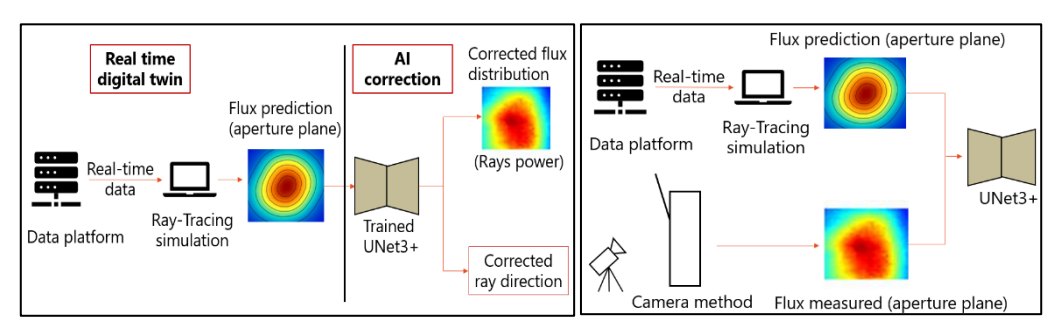


Figure 1. Schematic of the training loop, working in parallel with the camera method for calibration (left) and schematic of the operation loop, getting corrected flux maps and using only the DT (right)

2.1 Digital twin

Digital twins have been used in the past to accurately simulate real world environments [15]. It is possible to find a wide variety of applications in bibliography, thanks to the increase in computing power, the improvement of data science and the growth of AI techniques during the last decade. Some of these examples are based on such varied physical systems like conventional energy plants [16] or even solar thermal designs [17]. However, there was a knowledge gap in digital twins for SPT plants' operation and monitoring.

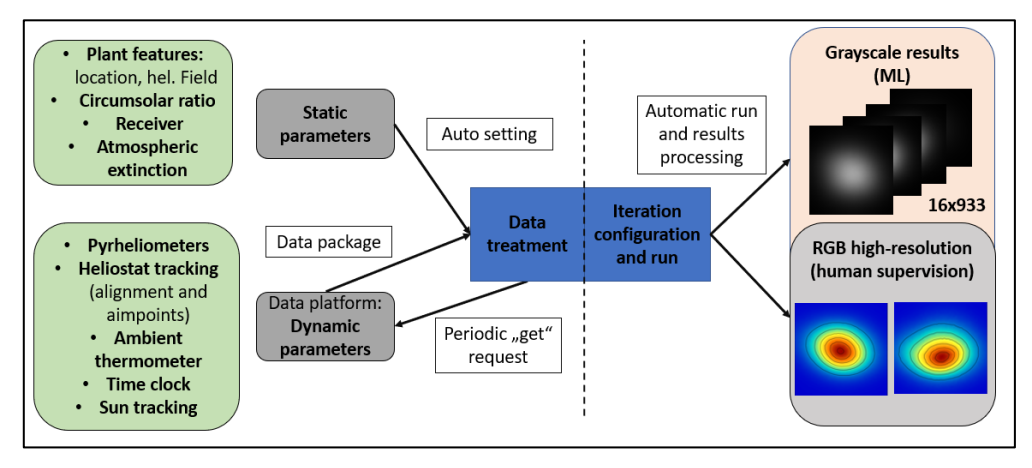


Figure 2. Detailed schematic of the digital twin internal workflow

In order to cover this gap, the DT of the Solar Tower Jülich was developed. The model consists of a library of Python functions, represented by the blue square in Figure 2, making it

possible to operate either manually, for testing and configuring specific desired conditions, or automatically, cloning (in real time) the same working conditions than in the real plant, taking the signal from the sensors located there.

As shown in the figure above, the set of functions is connected at the same time to the data platform (gray elements) and to STRAL, the DLR-built ray-tracer (red and gray squares). This connection is set by the operator and it is continuous until the user stops it, so there is a complete path from back-end to front-end, where the data can circulate in both directions. As a result, the real-time situation of the physical system (modelled by the green elements), chronologically stored in the data platform, can modify the configuration of the simulation. In the case of a complete data platform (DP), this could also occur in the other direction: the modifications in simulation environment can modify the state of the physical system. Currently, the data platform in STJ is under development, so the number of sensor signals is limited and the data itinerance from the computing system to the physical system too. With the completion of the data platform, these two limits will disappear, as the library is already prepared to operate with all the inputs needed for the simulation or for the real SPT operation.

In terms of usage, the operator has to install the complete library of Python functions, as well as STRAL and also has to establish connection with the data platform. The architecture of the library allows connection to every data platform protected by OAuth/OAuth2 protocol. At this time, the ray-tracer has to be STRAL, as the heliostats models and the translation of the parameters from the DP is set for this software. When all the software has been installed, two operation modes are possible: automatic and manual.

On the one hand, in the automatic operation mode, the operator has to run the main function of the library every time a new flux density measurement has to be performed. Automatically, the simulation will be configured with the available real-time data from the data platform and the flux map will be obtained in ".png" format with 1940x1406 px resolution in grayscale and RGB formats. The results will be saved in a folder called "results" automatically created and they will be labelled with the date and time of the measurement. In order to supervise the correct configuration of the time step, the digital twin uses STRAL user interface as graphic representation, updating in real time the modified parameters (e.g. focused heliostats or DNI). In the case of this operation mode, the power plant will be automatically created before the first time step using the "static parameters" from Figure 2 (currently defined for STJ). Then, the "dynamic parameters" will be refreshed for every simulation using iterative queries.

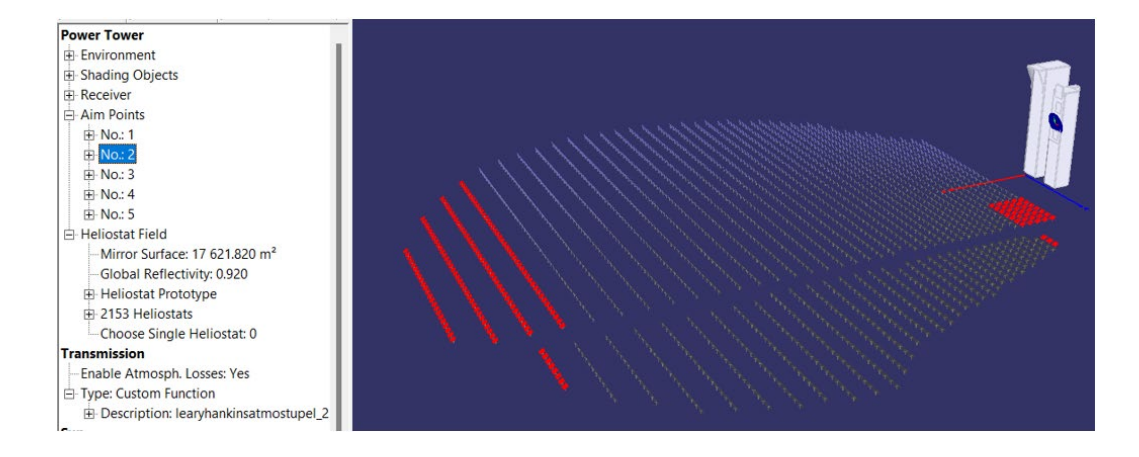


Figure 3. Graphic representation of the time-step in STRAL GUI usable by operator. The heliostats are automatically defocused with the info from the data platform (highlighted in red)

On the other hand, it is also possible to use this model manually, uploading data to the server and, then, running the main function. For this operation mode, the user has to interact with the "post request" function in the Python environment. In the post sentence all the data

required for the simulation configuration have to be included as a header in JSON format. Then, one can run the main function and the same process as in the automatic operation mode will be performed, getting the overwritten data from the data server. This mode can be really interesting for quick testing of design-stage plants or for reproducing old experiments in order to check accuracy of the model or the best parameters for the simulation.

2.2 Machine learning correction module

The outputs of the digital twin are a high-resolution image (1940x1406 px) showing the flux density distribution in a flat receiver and a text file with the information of all the rays intersecting the flat plane studied (point of the intersection, direction of the ray, power carried by the ray and heliostat of origin). These results will obviously contain inaccuracies, due to the high correlation of the quality of outputs and inputs in simulations. In every experimental environment the measured parameters are biased either by sensors and measurement techniques or by the intrinsic error in mathematical models (e.g. tracking error or atmospheric extinction), so a non-perfect quality can be expected in results of the digital twin. The machine learning module is thought to solve this issue for the task shown in Figure 4 with broad application in industrial environments.

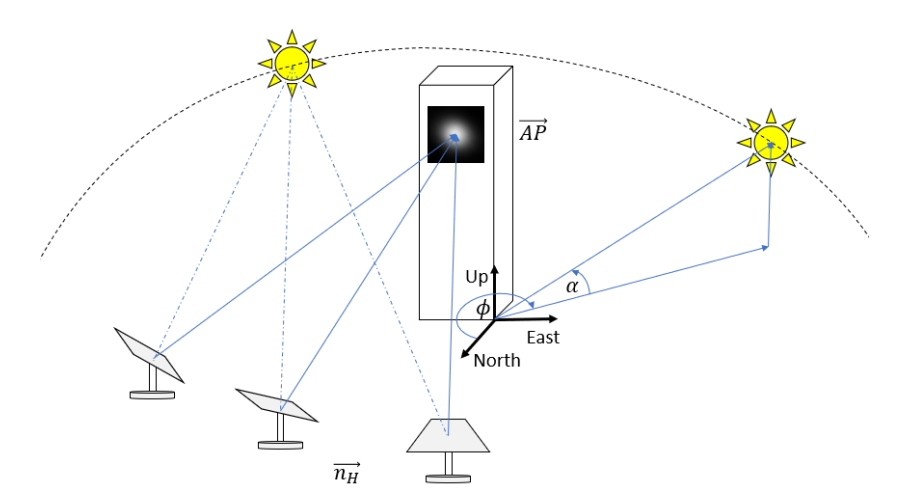


Figure 4. Sketch of the simplified problem initially solved by the pre-trained version of Real-TIME 3DT.

In order to apply this correction, the well-known UNet [18] graph neural net has been used. This algorithm consists of a sequence of five layers of convolutional filters ordered in an encoder-decoder architecture and receives pairs of images of 256x256 px as an input originally with three channels (RGB). The architecture of the model has been tuned for this specific case, increasing the depth to six convolutional layers, changing the number of channels to one and allowing the possibility of introducing images up to 512x512 px. The original loss function (binary cross entropy) has been also substituted by mean-square error (MSE) loss. The aim of all these changes is the increase of data obtention from each image, the improvement in computing time and the acceptance of multiclass and more complex data, respectively.

The neural-net based correction is designed in order to map from simulated flux distributions (in real-time in the digital twin) to distributions with the quality of camera methods, which has been proven to be higher due to considering real perturbations like cloud transients or atmospheric extinction. As detailed in equation (1), this is a complex problem in terms of dimensional analysis, dependent on sun position (azimuth and elevation: α, ϕ), DNI, number and position of focused heliostats $(\overrightarrow{n_H})$, aimpoints (\overrightarrow{AP}) , atmospheric extinction (E) and tracking errors matrix (\overrightarrow{TE}) , defined by the 2-axis angular tracking error and the 2-axis linear deformation of the 2153 heliostats' structure in STJ).

$$FDM = f(\alpha, \phi, DNI, \overrightarrow{AP}, \overrightarrow{n_H}, E, \overrightarrow{TE})$$
 (1)

All of these parameters have to be learned intrinsically by the neural net, trying to relate the combination of all of them to the resulting image. For example, in the Figure 5, it is possible to check the functional relation between the date and time of the experiment and the light spot anatomy in simulation environment. In other words, it is possible to co-relate the shape and central point of the light beam to a determined DNI, azimuth and elevation values (i.e. date and time). With a sufficiently large and varied dataset, the neural net can learn the image mapping related to these variables, as the behaviour is periodical during the years.

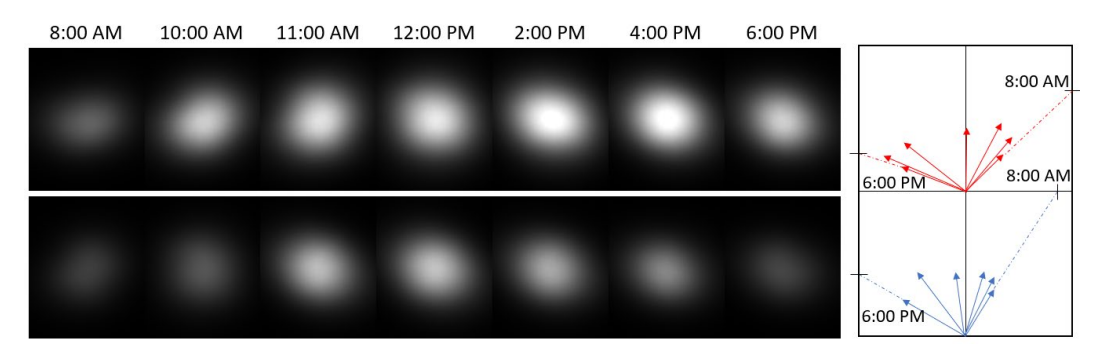


Figure 5. Simulated light spot in the evaluation plane of the experiments (left). Direction and length of the longest beam's radius (right). Upper row for 02-07-14 and lower row for 09-09-14.

On the other hand, if more than one aimpoint and the individual effects of each heliostat and its four tracking errors had to be considered in the same training step, the dataset would be so large that it would increase the computing time enormously. Then, the method wouldn't be interesting for the industry, as millions of combinations would have to be tested.

As a consequence, a training methodology is presented in this work, based on dividing the training process into several pre-training steps to teach the model the different functional dependencies gradually. Firstly, the model has been pre-trained comparing 15000 pairs of images obtained from scattered situations during 3 years, simulated using real atmospheric data from DLR's experiments between 2014 and 2016. Moreover, in order to perform these simulations, the heliostat field has been divided into 16 groups and they have been disconnected group-wise randomly for the dataset generation. Therefore, it is possible for the net to learn the effect of each group (in incident power and beam shape) for the FDM thanks to the greater variability of the images in the dataset. In order to learn also the effect of the tracking errors, the label of each training pair is obtained from simulations with tracking errors, whereas the input of each pair is the output of simulations without tracking error. It has been possible to generate those combinations of parameters thanks to the usage of the digital twin in manual mode.

With this method, it is possible to ensure that the pre-training of the neural net has been successful if it creates an image with the correct centre point, size of the light beam and intensity, giving as an input a flux map obtained from simulations without tracking errors. In this case, the model will have learned the effect of sun position, DNI and tracking error. Therefore, for the later training, the neural net will have to learn only the effect of different aimpoints and real atmospheric extinction. This way, thanks to decoupling variables, the dimensionality and, hence, the number of data samples required, are simplified.

3. Results

In this paper, the result of the first step of training of the tuned UNet are presented. This pretraining has been performed under a semi-controlled situation in terms of parameters. On the one hand, the stochastic number of heliostats focused is decomposed in 16 different areas with equivalent power contribution in the central receiver. On the other hand, the pre-training has been limited to one aimpoint, fitting perfectly the requirements for cavity receiver flux maps, but not for open volumetric receivers. Furthermore, the heliostat surface modelling is based on the last deflectometric measurement campaign in STJ and other static parameters, like the circumsolar ratio (CSR) of the Sun, optimal number of rays and atmospheric extinction models are obtained from the optimal configurations shown in ref. [19]. This will be the default configuration of the digital twin, as it has been tested against real experiments.

Under these conditions, and leaving the variations of the rest of parameters for future training steps, the neural net has been trained and tested with the dataset mentioned above, in order to check how well it is able to predict and correct tracking error effects in FDM. In this section, four main indicators have been used as metrics to quantify the performance of the neural net: the distribution of the absolute normalized intensity difference against the reference value (with tracking error) after the correction, the difference between the output and input of the neural net (Figure 7), the mean square error (MSE) value (used as loss function in the training) and a custom accuracy function (Figure 6). This metric is based on the comparison of the power absorbed by the target in the label and in the prediction, assessing pixel-wise this difference [13], eq. (14). These four values will show the effectiveness of the neural net in predicting intensities, positions and shapes of the light beam. In order to study the following graphs, the authors describe the behavior of the dark colored curves, what correspond to the softened functions. The light colored curves represent the exact epoch losses and accuracies, but these values are not representative in the analysis of these parameters' trends.

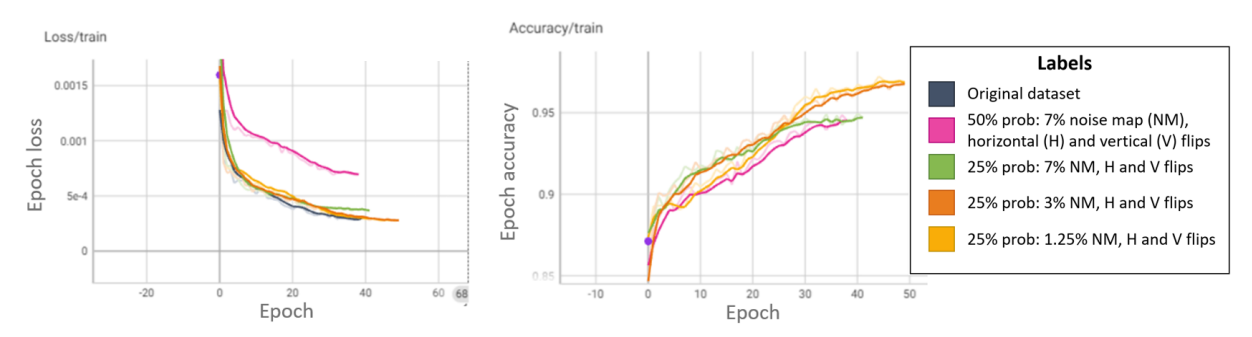


Figure 6. Evolution of the epoch loss (left) and epoch custom accuracy value (right) in Y-axis against the number of epochs in X-axis for different training augmentation techniques.

In the last graph it is possible to observe two families of curves: the first one showing a set of losses for the tuned U-Net model presented in this work and the second, its accuracy for predicting the synthetic dataset generated with real measurements from STJ. In the five cases presented here, the model is converging, but the performance varies slightly. The reason is the augmentation technique used to increase the generalization capabilities of the model. Augmentation is defined as the enhancement or enrichment of the dataset by including synthetic features that originally were not appearing. In this case, random horizontal and vertical flips were applied to the dataset with different probabilities, as well as random noise maps (with an amplitude of 1.25% to 7% of the peak radiation case) to make the dataset more similar to real measurements, with background radiation and different noise sources.

In order to compare the behaviour of the model and how it is able to generalize, the original dataset was used for a complete training, giving as a result a loss limit of 3e-4 (dark blue curve). Then, rotations and noise maps (7% amplitude) were each applied to a random 50% of the samples, giving the pink curve as a result. The randomization of the data batch was big enough to affect the learning behaviour of the model. Reducing this probability of transformations to 25% the green curve was obtained. There, the learning was almost as good as in the original case, with a loss limit of 4e-4, but the noise was still affecting the accuracy of the model. Then, noise map amplitude was reduced to 3%, what gives the yellow curve as a result. Finally, with a noise of 1.25% and transformations applied independently to 25% of the samples, the orange curve was obtained. There, the model performed as good as with the original data batch (training epoch loss of 3e-4), but increasing the generalization possibilities, as it

learned the three transformations applied and it was able to reproduce them. In parallel, the accuracy was also studied during the whole training process and the results were satisfactory: 97.5% of the power was included in the prediction.

Moreover, analysing the variation of these two metrics also provides information about the performance of the model. The training loss has been decreased from 0.002 to 0.0003, so the difference between images is decreased one order of magnitude and the accuracy improves a 12% (from 85% to 97.5%).

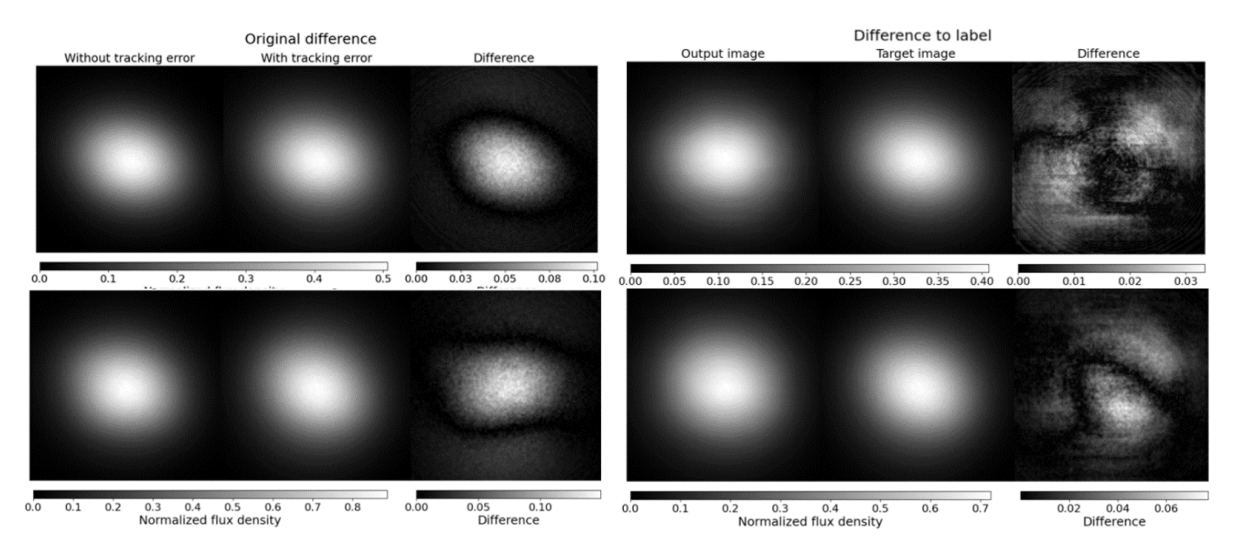


Figure 7. Original difference between ideal and realistic simulations and difference after correction for medium DNI (2019-05-07@13:43:59) in 1st row and high DNI case below (2018-06-14@12:14:52)

In the figure above it is possible to check how the model performs the corrections for medium and high irradiation cases obtained from past experiments. In the original cases (left column), the peak differences are between 20 and 25% of the peak normalized flux density value, i.e. 0.1 out of 0.5 and 0.15 out of 0.8, respectively. Furthermore, this difference is mostly concentrated in the centre of the light spot, leading to a considerable overestimation in the ideal case and severe consequences in the measurement. Moreover, the MSE for the high intensity value is 0.0013 in normalized scale and 0.0006 for the medium intensity case. These considerable differences show the importance of the tracking error in simulation results.

In the right column it is possible to check the result of the correction. First of all, the grey-scale bars show that peak differences are now below a 10% of the peak values (0.03 out of 0.4 and around 0.06 out of 0.7, respectively). Moreover, in the flux distribution, the results also improve, as the error is now distributed and not concentrated in the hottest spot. A distributed variation of the error lead to better approximations and less dangerous results, as the values of heat flux are lower in the surroundings. Finally, the MSE has decreased one order of magnitude in the high intensity case, reaching values of 0.00028 (80% of improvement). For the medium intensity case, the MSE has decreased until 8.3e-5 (an order of magnitude again).

4. Outlook and perspectives

Considering the results after the analysis of the four metrics, the method has shown an outstanding performance. Losses/MSE have improved up to 80%, reducing one order of magnitude. Thanks to this, the uncertainties are better distributed (reducing hot spot inaccuracies) and the accuracy in terms of power collected in the receiver have reached values up to 97.5%. Moreover, the performance has been shown for different intensities, showing that the model is able to predict different regimes. Other state-of-the-art deep-learning approaches like iDLR [20] or the model presented by Kuhl et al. [21] have recently achieved accuracies up to 92% or 90%, respectively. Although these results are currently obtained for simulated flux maps,

the usage of measured flux maps from the aperture plane of any receiver in the training step (sim2real) enable universal non-disruptive measurement. The corrected flux maps are obtained from the trained neural network (connected to the DT environment), which means that the aperture plane does not need to be covered for flux measurements with state-of-the art accuracies. Furthermore, the corrected flat fluxes can be projected to any geometry (cylindrical or hemispherical cavities, curved surfaces), but this module is out of the scope of this work.

Among the future lines, the results for very low intensities have to be shown. Due to the reduced length of this paper, this couldn't be included, but the corrections are performing quantitatively similar to the cases shown in this work (medium-high intensities). Finally, the already pre-trained model (with tracking error prediction) has to be used for sim2real inference, by training it again with real images from experiments against realistic simulations.

Data availability statement

Data are not still available in online repositories. The different interested parties should discuss about the way in which this software and datasets will be (or not) shared.

Author contributions

Conceptualization, methodology, software, investigation, writing - original draft and visualization: S.D.; writing-review and edition: C.R; supervision: C.R. and B.H.; funding acquisition: K.W.

Competing interests

The authors declare that they have no competing interests.

Funding

This project has been funded by the European Union (HORIZON MSCA Doctoral Network, Project number 101072537).

References

- [1] F. J. Collado and J. Guallar, "A review of optimized design layouts for solar power tower plants with campo code," *Renewable and Sustainable Energy Reviews*, vol. 20, pp. 142-154, 2013, doi: 10.1016/j.rser.2012.11.076.
- [2] R. Schappi *et al.*, "Drop-in fuels from sunlight and air," *Nature*, vol. 601, no. 7891, pp. 63-68, Jan 2022, doi: <u>10.1038/s41586-021-04174-y</u>.
- [3] A. H. Alami *et al.*, "Concentrating solar power (CSP) technologies: Status and analysis," *International Journal of Thermofluids*, vol. 18, p. 100340, 2023.
- [4] S. A. Zavattoni *et al.*, "Synhelion absorbing gas solar receiver Design advancement," *AIP Conference Proceedings*, vol. 2815, no. 1, 2023, doi: 10.1063/5.0149049.
- [5] M. I. Alam, M. M. Nuhash, A. Zihad, T. H. Nakib, and M. M. Ehsan, "Conventional and Emerging CSP Technologies and Design Modifications: Research Status and Recent Advancements," *International Journal of Thermofluids,* vol. 20, 2023, doi: 10.1016/j.iift.2023.100406.
- [6] M. Röger, P. Herrmann, S. Ulmer, M. Ebert, C. Prahl, and F. Göhring, "Techniques to Measure Solar Flux Density Distribution on Large-Scale Receivers," *Journal of Solar Energy Engineering*, vol. 136, no. 3, 2014, doi: 10.1115/1.4027261.

- [7] R. Osuna, R. Morillo, J. M. Jiménez, and V. Fernández-Quero, "Control and Operation Strategies in PS10 Solar Plant," in *13th SolarPACES*, Sevilla, Spain, Jun. 20-23 2006, pp. 1-5
- [8] M. Offergeld, M. Röger, H. Stadler, P. Gorzalka, and B. Hoffschmidt, "Flux density measurement for industrial-scale solar power towers using the reflection off the absorber," presented at the SOLARPACES 2018: International Conference on Concentrating Solar Power and Chemical Energy Systems, 2019.
- [9] M. Thelen, C. Raeder, C. Willsch, and G. Dibowski, "A high-resolution optical measurement system for rapid acquisition of radiation flux density maps.," in *SolarPACES 2016*, Abu Dhabi, UAE, 2016, vol. 1850, no. 12: AIP Publishing, 2017, doi: 10.1063/1.4984534.
- [10] G. von Tobel, C. Schelders, and M. Real, "Concentrated solar-flux measurements at the IEA-SSPS solar-central-receiver power plant, Tabernas Almeria (Spain). Final report. Technical report No. 2/82," 1982.
- [11] S. Ulmer, E. Lüpfert, M. Pfänder, and R. Buck, "Calibration corrections of solar tower flux density measurements," *Energy,* vol. 29, no. 5-6, pp. 925-933, 2004, doi: 10.1016/s0360-5442(03)00197-x.
- [12] M. R. Rodríguez-Sánchez, A. Sánchez-González, and D. Santana, "Field-receiver model validation against Solar Two tests," *Renewable and Sustainable Energy Reviews,* vol. 110, pp. 43-52, 2019/08/01/ 2019, doi: https://doi.org/10.1016/j.rser.2019.04.054.
- [13] M. Kuhl, M. Pargmann, M. Cherti, J. Jitsev, D. M. Quinto, and R. Pitz-Paal, "In-Situ UNet-Based Heliostat Beam Characterization Method for Precise Flux Calculation Using the Camera-Target Method," ed: Research Square, 2024.
- [14] I. Miadowicz, D. M. Quinto, R. Pitz-Paal, and M. Felderer, "An action research study on the digital transformation of concentrated solar thermal plants," *Solar Energy Advances*, vol. 5, p. 100102, 2025/01/01/ 2025, doi: https://doi.org/10.1016/j.seja.2025.100102.
- [15] K. Arafet and R. Berlanga, "Digital Twins in Solar Farms: An Approach through Time Series and Deep Learning," *Algorithms*, vol. 14, no. 5, p. 156, 2021. [Online]. Available: https://www.mdpi.com/1999-4893/14/5/156.
- [16] J. Yu, P. Liu, and Z. Li, "Hybrid modelling and digital twin development of a steam turbine control stage for online performance monitoring," *Renevable and Sustainable Energy Reviews*, vol. 133, 2020.
- [17] T. I. Zohdi, "A machine-learning digital-twin for rapid large-scale solar-thermal energy system design," *Computer Methods in Applied Mechanics and Engineering*, 2023.
- [18] O. Ronneberger, P. Fischer, and T. Brox, "U-Net: Convolutional Networks for Biomedical Image Segmentation," *ArXiv*, vol. abs/1505.04597, 2015.
- [19] B. Belhomme, R. Pitz-Paal, P. Schwarzbözl, and S. Ulmer, "A new fast ray tracing tool for high-precision simulation of heliostat fields," *Journal of Solar Energy Engineering*, vol. 131, 2009, doi: 10.1115/1.3139139.
- [20] J. Lewen, M. Pargmann, M. Cherti, J. Jitsev, R. Pitz-Paal, and D. M. Quinto, "Inverse Deep Learning Raytracing for heliostat surface prediction," *Solar Energy,* vol. 289, p. 113312, 2025/03/15/ 2025, doi: https://doi.org/10.1016/j.solener.2025.113312.
- [21] M. Kuhl, M. Pargmann, M. Cherti, J. Jitsev, D. Maldonado Quinto, and R. Pitz-Paal, "Flux density distribution forecasting in concentrated solar tower plants: A data-driven approach," *Solar Energy*, vol. 282, p. 112894, 2024/11/01/ 2024, doi: https://doi.org/10.1016/j.solener.2024.112894.